

SIMULATION OF STYRENE POLYMERIZATION IN ARBITRARY CROSS-SECTIONAL DUCT REACTORS BY BOUNDARY-FITTED COORDINATE TRANSFORMATION METHOD

M. A. Isazadeh

Department of Chemical Engineering, University of Petroleum Industry
Ahwaz, Iran

(Received: February 19, 2000 - Accepted in Final Form: October 21, 2001)

Abstract The non-orthogonal boundary-fitted coordinate transformation method is applied to the solution of steady three-dimensional conservation equations of mass, momentum, energy and species-continuity to obtain the laminar velocity, temperature and concentration fields for simulation of polymerization of styrene in arbitrary cross-sectional duct reactors. Variable physical properties (except for specific-heat), viscous heat dissipation and free-convection effects are considered in modeling while axial diffusion is ignored. The conservation equations originally written in Cartesian coordinates are parabolized in the axial direction and then transformed to the non-orthogonal curvilinear coordinates to handle arbitrary duct geometries. The transformed equations are discretized by the control-volume finite-difference approach in which the convective and diffusive terms are handled by the upwind-difference and central-difference approximation schemes respectively. Results are obtained for eight different geometries. The results show that not a specific geometry is in general superior to conventional circular duct reactors for the highest conversion of the chemical reaction under study, considering also the least pressure-drop in the reactors.

Keywords Boundary-Fitted Coordinate, Styrene Polymerization, Arbitrary Cross-Sectional Duct Reactors

چکیده روش غیر متعامد انتقال مختصات دربرگیرنده حدود اشکال هندسی برای حل معادلات یکنواخت سه بعدی بقاء جرم، مومنتم، انرژی و تداوم اجزا بکال ر برده شده تا توزیع سرعت در جریان آرام و نیز توزیع دما و غلظت برای مشابه سازی پلیمریزاسیون استایرین در راکتورهای با سطوح مقطع دلخواه بدست آید. خواص فیزیکی متغیر (غیر از گرمای ویژه)، هدر رفتگی انرژی و اثرات کنوکسیون آزاد در مدل ریزی در نظر گرفته شده؛ درحالیکه از نفوذ محوری صرفنظر شده است. معادلات بقاء که در ابتدا در مختصات کارتزین نوشته شده در جهت محوری پارابلیزه شده و سپس به سیستم مختصات غیر متعامد منحنی-خطی انتقال می یابند تا اشکال هندسی دلخواه را در برگیرند. معادلات انتقال یافته با شیوه کنترل حجمی در روش تفاضلات متناهی، توزیعی گسسته یافته بطوریکه در آن به جملات کنوکسیون و نفوذ با متدهای مخصوص بخود برخورد می شود. نتایج بدست آمده برای هشت شکل هندسی مختلف نشان می دهد که هیچ شکل هندسی بخصوصی در حالت کلی بر راکتورهای با سطوح مقطع دایره ای از نظر بیشترین مقدار تبدیل در واکنش شیمیایی مورد مطالعه و حداقل افت فشار در راکتور، امتیاز ندارد.

INTRODUCTION

The purpose of this paper is to provide simultaneous heat and mass transfer solution of steady laminar flow polymerization of styrene in arbitrary cross-sectional duct reactors.

A review of literature in this area reveals that the previous investigations carried-out for simulation of polymerization of styrene are only in conventional cylindrical reactors. Sala et al. [1] analyzed styrene polymerization by solving the steady, two dimensional conservation equations

numerically using the upwind scheme for convective terms and the stream-function/vorticity approach. The finite difference equations were solved by Gauss-Seidel technique. The fluid was assumed to be Newtonian. Polystyrene, however, is a non-Newtonian fluid. Variable (temperature-dependent) physical properties were used. The viscous heat generation was disregarded. A simple first-order kinetics along with a constant molecular weight of 70,000 was employed. The influence of inlet feed concentration, inlet temperature and feed-rate on the temperature distribution in adiabatic and

isothermal tubular reactors was analyzed. It was concluded that adequate control of the polymerization can be achieved by maintaining the tube wall temperature below the inlet feed temperature to inhibit thermal runaway.

Wyman et al. [2] introduced an approximate model to calculate the number and weight-average molecular weights of the polymer being produced in a continuous steady-state tubular reactor from the zeroth, first and second moments of radical and polymer distributions. The partial differential equations describing temperature, velocity and composition were written considering axial symmetry and incompressible laminar flow in a cylindrical tube allowing for variable viscosity and conductivity. The reaction rate constant was of Arrhenius type in which the so-called gel effect was also taken into account. The pressure drop in the tube was obtained from the equation of motion. Radial convection, axial conduction and viscous heating of polymer in the energy balance equation were neglected. The radial and angular components of velocity were ignored in the equation of motion. The partial differential equations were solved numerically using the classical explicit finite-difference method.

Husain et al. [3] made a computational study of bulk thermal polymerization of styrene in a tubular reactor in which the fluid rheology was represented by a power-law model. They considered the polymer to be a non-diffusing specie and neglected radial velocities. They also neglected the axial diffusion of mass and energy. They took into account the gel effect following Hui et al [4]. Finite differencing radially and solving the resulting equations using a fourth-order Runge-Kutta-Gill routine solved the system of differential equations.

Valsamis et al. [5,6] used piston flow and segregated flow models for the polymerization of styrene in tubular reactors. Experiments were performed in a helically coiled tube with a length of 14.6 m and a diameter of 0.46 cm. Running pure thermal styrene polymerization at 160 degrees Celsius yielded a conversion of 15% in 5.15 minutes residence time.

Chen et al [7,8] determined the residence time washout function theoretically by means of flow models and experimentally by inert tracer techniques. Introducing steady mass, momentum and energy transport equations for laminar axisymmetric flow in cylindrical coordinates using fully developed

velocity profile in axial direction. The mass diffusion and heat conduction in axial direction were ignored. The viscous heating effect was also ignored. The fluid was assumed Newtonian. The polymer was considered to be non-diffusing. The kinetic rate constants were obtained from Hui et al. [4], while the physical property data were obtained from various sources. The partial differential equations were solved by the method of lines (MOL) in which the equations were approximated by a set of initial value problems (IVP) in ordinary differential equations that were then discretized using finite differences and solved by IVP solvers. The model predicted axial and radial velocity profiles which were subsequently used in a tracer model that consisted of the unsteady, two-dimensional convective diffusion equation. The solution of this model evaluated at the tube outlet provided the residence time washout function. Experimental measurements were made to verify the theoretical model for residence time distribution using toluene as a nonreactive inert tracer. The measured washout function confirmed the presence of velocity profile elongation. Molecular weight of polymer was also calculated using the approach based on the zeroth, first and second moments of radical and polymer distributions.

Kleinstreuer and Agarwal [9,10] solved the two-dimensional equations governing the thermal polymerization of styrene at steady state in laminar flow in a straight circular duct assuming axial-symmetry and power law model for liquid behavior. They neglected the body force term but considered variable physical properties and a developing flow with parabolic velocity profile at inlet. They obtained the kinetic rate constants from Hui et al. [4] and the data for physical properties from various sources. They employed control volume approach for discretization and used a software package using the SIMPLE algorithm to obtain the results. They analyzed a simple tube as a representation of the shell-and-tube type configuration. They generated stability plots by computer experimentation varying the effective system parameters and concluded that a small tube up to a radius of 2 cm could be effectively used to carry out styrene polymerization. However, as the tube radius increases, the problem of thermal runaway and flow elongation make the operation unfeasible.

The objective of this study is to employ a numerical solution method [11] based on non-orthogonal boundary-fitted coordinate transformation and make any developments required to apply to the simulation of polymerization of styrene in complex geometry cross-sectional duct reactors. Results are obtained for eight different geometries and for five different sets of operating conditions.

THE MATHEMATICAL MODELLING

The strongly conservative form [12] of the steady overall continuity, momentum energy and species continuity equations are expressed as follows:

The Overall Continuity Equation

$$(\nabla \cdot \rho v) = 0 \quad (1)$$

The Momentum Equation

$$-(\nabla \cdot \rho v v) - \nabla P - (\nabla \cdot \tau) + \rho g = 0 \quad (2)$$

The Energy Equation

$$-(\nabla \cdot \rho C_p T v) - (\nabla \cdot q) - (\tau : \nabla v) + Q_R = 0 \quad (3)$$

The Reactant Continuity Equation

$$(\nabla \cdot \rho m_A v) = (\nabla \cdot \rho D_A \nabla m_A) - R_A \quad (4)$$

The coordinate axes selected for the Cartesian domains are shown in Figure 1.

The Constitutive Equation The rheological behavior of polystyrene can be adequately expressed by power-law non-Newtonian model [3,9,10]. For power-law model the stress-tensor is related to the rate-of-strain tensor [13] by the following relationship:

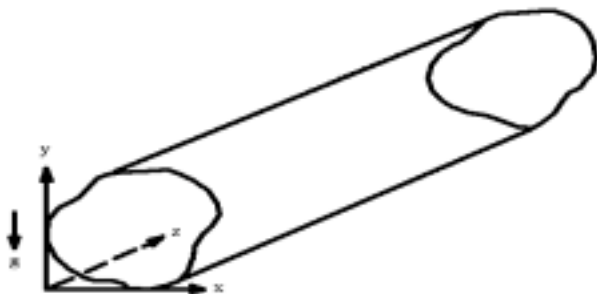


Figure 1. Arbitrary cross-sectional duct in Cartesian coordinates.

$$\tau_{ij} = -\mu \left| \sqrt{\frac{1}{2} (\Delta_{ij} : \Delta_{ij})} \right|^{n-1} \Delta_{ij} \quad (5)$$

The Parabolized Governing Equations in Cartesian Coordinates

The overall continuity equation

$$\frac{\partial}{\partial x}(\rho u) + \frac{\partial}{\partial y}(\rho v) + \frac{\partial}{\partial z}(\rho w) = 0 \quad (6)$$

The Momentum Equations

x-Component

$$\begin{aligned} \frac{\partial}{\partial x}(\rho u^2) + \frac{\partial}{\partial y}(\rho v u) + \frac{\partial}{\partial z}(\rho w u) = \\ -\frac{\partial P}{\partial x} - \left(\frac{\partial \tau_{xx}}{\partial x} + \frac{\partial \tau_{yx}}{\partial y} \right) \end{aligned} \quad (7)$$

y-Component

$$\begin{aligned} \frac{\partial}{\partial x}(\rho u v) + \frac{\partial}{\partial y}(\rho v^2) + \frac{\partial}{\partial z}(\rho w v) = \\ -\frac{\partial P}{\partial y} - \left(\frac{\partial \tau_{xy}}{\partial x} + \frac{\partial \tau_{yy}}{\partial y} \right) - (\rho - \rho_a) g \end{aligned} \quad (8)$$

z-Component

$$\begin{aligned} \frac{\partial}{\partial x}(\rho u w) + \frac{\partial}{\partial y}(\rho v w) + \frac{\partial}{\partial z}(\rho w^2) = \\ -\frac{dP}{dz} - \left(\frac{\partial \tau_{xz}}{\partial x} + \frac{\partial \tau_{yz}}{\partial y} \right) \end{aligned} \quad (9)$$

The Energy Equation

$$\begin{aligned} \frac{\partial}{\partial x}(\rho C_p T u) + \frac{\partial}{\partial y}(\rho C_p T v) + \frac{\partial}{\partial z}(\rho C_p T w) = \\ \frac{\partial}{\partial x} \left(k \frac{\partial T}{\partial x} \right) + \frac{\partial}{\partial y} \left(k \frac{\partial T}{\partial y} \right) + M \Phi_v + (-\Delta H) R_A \end{aligned} \quad (10)$$

The Reactant Continuity Equation

$$\begin{aligned} \frac{\partial}{\partial x}(\rho m_A u) + \frac{\partial}{\partial y}(\rho m_A v) + \frac{\partial}{\partial z}(\rho m_A w) = \\ \frac{\partial}{\partial x} \left(\rho D_A \frac{\partial m_A}{\partial x} \right) + \frac{\partial}{\partial y} \left(\rho D_A \frac{\partial m_A}{\partial y} \right) - R_A \end{aligned} \quad (11)$$

The pressure, P in the above equations is dynamic-pressure due to the introduction of

buoyancy term in the “y” momentum equation. In cases of negligible buoyancy effect, P would be the total pressure defined as hydrostatic plus dynamic pressures. The term M is the apparent viscosity for the power-law non-Newtonian fluid.

The Boundary Conditions

Inlet (@z=0) Axial Velocity A uniform entrance velocity profile is specified at inlet:

$$w = w_{inlet} \quad (12)$$

Transverse Velocities It is assumed that there is no secondary flow at inlet:

$$u = 0, \quad v = 0 \quad (13)$$

Temperature A uniform temperature-profile is specified at inlet:

$$T = T_{inlet} \quad (14)$$

Reactant Weight Fraction For an unconverted reactant at inlet:

$$m = 1 \quad (15)$$

Walls of the Duct Axial Velocity No slip-condition is assumed on the walls of the duct:

$$w = 0 \quad (16)$$

Transverse Velocities

$$u = 0, \quad v = 0 \quad (17)$$

Temperature For a constant wall- temperature:

$$T = T_{wall} \quad (18)$$

Reactant Weight-Fraction The material does not, move through the wall:

$$\frac{\partial m}{\partial n} = 0 \quad (19)$$

Outflow Condition (@z = L) For the parabolized governing equations used here no downstream boundary conditions are required.

THE BOUNDARY-FITTED METHOD

The development of the boundary-fitted coordinate systems brought about the coordinate transformation of the physical domain, such as Cartesian coordinates

to the curvilinear coordinates so that all the boundaries match the coordinate lines in the new system and the need to interpolate the boundary conditions as practiced before is eliminated [14,15].

The curvilinear coordinate system may be either orthogonal or non-orthogonal in the sense of the mesh generated over the physical-domain. In this study the non-orthogonal method is applied to obtain solutions of the present three-dimensional problem in irregular cross-sectional ducts.

TRANSFORMATION OF GOVERNING PDE'S

It is necessary to transform the partial-differential equations under consideration into the new coordinate variables before being discretized. In general, the transformation operation generates additional terms in the governing equations so that these equations become more complicated upon transformation. The physical Cartesian velocities are retained as the dependent variables in transformation. However, the contra-variant velocity components also take part in the structure of the transformed equations. The transformed equations are as follows:

The Overall Continuity Equation

$$\frac{\partial}{\partial \zeta}(\rho U) + \frac{\partial}{\partial \eta}(\rho V) + \frac{\partial}{\partial \sigma}(\rho W) = 0 \quad (20)$$

The Momentum Equations

x-Component

$$\begin{aligned} \frac{\partial}{\partial \zeta}(\rho u U) + \frac{\partial}{\partial \eta}(\rho u V) + \frac{\partial}{\partial \sigma}(\rho u W) = \\ - \frac{\partial}{\partial \zeta} [y_{\eta}(\hat{\tau}_{xx}) - x_{\eta}(\hat{\tau}_{yx})] - \frac{\partial}{\partial \eta} [x_{\zeta}(\hat{\tau}_{yx}) - y_{\zeta}(\hat{\tau}_{xx})] \\ - [y_{\eta} P_{\zeta} - x_{\zeta} P_{\eta}] \end{aligned} \quad (21)$$

y-Component

$$\begin{aligned} \frac{\partial}{\partial \zeta}(\rho v U) + \frac{\partial}{\partial \eta}(\rho v V) + \frac{\partial}{\partial \sigma}(\rho v W) = \\ - \frac{\partial}{\partial \zeta} [y_{\eta}(\hat{\tau}_{xy}) - x_{\eta}(\hat{\tau}_{yy})] - \frac{\partial}{\partial \eta} [x_{\zeta}(\hat{\tau}_{yy}) - y_{\zeta}(\hat{\tau}_{xy})] \\ - [x_{\zeta} P_{\eta} - x_{\eta} P_{\zeta}] - J(\rho - \rho_a)g \end{aligned} \quad (22)$$

z-Component

$$\frac{\partial}{\partial \zeta}(\rho w U) + \frac{\partial}{\partial \eta}(\rho w V) + \frac{\partial}{\partial \sigma}(\rho w W) = -\frac{\partial}{\partial \zeta}[y_\eta(\hat{\tau}_{xz}) - x_\eta(\hat{\tau}_{yz})] - \frac{\partial}{\partial \eta}[x_\zeta(\hat{\tau}_{yz}) - y_\zeta(\hat{\tau}_{xz})] - J \frac{dP}{d\sigma} \quad (23)$$

The Energy Equation

$$\frac{\partial}{\partial \zeta}(\rho C_p T U) + \frac{\partial}{\partial \eta}(\rho C_p T V) + \frac{\partial}{\partial \sigma}(\rho C_p T W) = \frac{\partial}{\partial \zeta} \left[\frac{\alpha}{J} k T_\zeta - \frac{\beta}{J} k T_\eta \right] + \frac{\partial}{\partial \eta} \left[\frac{\gamma}{J} k T_\eta - \frac{\beta}{J} k T_\zeta \right] + J M \hat{\Phi}_v + J(-\Delta H) \hat{R}_A \quad (24)$$

The Reactant Continuity Equation

$$\frac{\partial}{\partial \zeta}(\rho m_A U) + \frac{\partial}{\partial \eta}(\rho m_A V) + \frac{\partial}{\partial \sigma}(\rho m_A W) = \frac{\partial}{\partial \zeta} \left[\frac{\rho D_A}{J} \alpha m_\zeta - \frac{\rho D_A}{J} \beta m_\eta \right] + \frac{\partial}{\partial \eta} \left[\frac{\rho D_A}{J} \gamma m_\eta - \frac{\rho D_A}{J} \beta m_\zeta \right] - J \hat{R}_A \quad (25)$$

where $m = m_A$ for derivatives.

Boundary Conditions

Inlet ($@\sigma = 0$)

(i) **Axial Velocity** $w(\zeta, \eta) = w_{inlet}$ (26)

(ii) **Transverse Velocities** $u(\zeta, \eta) = 0, v(\zeta, \eta) = 0$ (27)

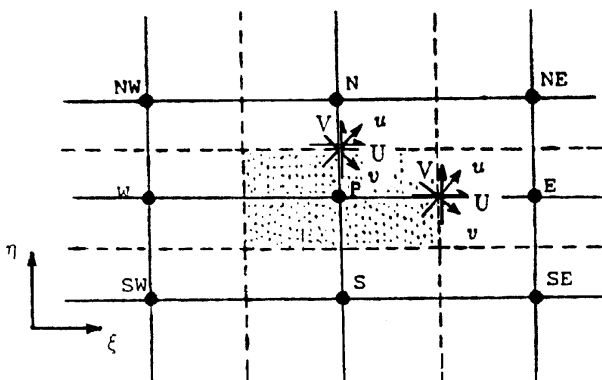


Figure 2. Grid arrangement adopted in Cartesian coordinates (transformed plane).

(iii) **Temperature**

$$T(\zeta, \eta) = T_{inlet} \quad (28)$$

(iv) **Reactant Weight-Fraction**

$$m(\zeta, \eta) = 1.0 \quad (29)$$

Walls of the Duct (i) **Axial Velocity**

$$w(\zeta, \eta) = 0 \quad \begin{matrix} 1 \leq \zeta \leq L_1 \text{ for } \eta = 1, M_1 \\ 1 \leq \eta \leq M_1 \text{ for } \zeta = 1, L_1 \end{matrix} \quad (30)$$

(ii) **Transverse Velocities**

$$u(\zeta, \eta) = 0 \quad v(\zeta, \eta) = 0 \quad \begin{matrix} 1 \leq \zeta \leq L_1 \text{ for } \eta = 1, M_1 \\ 1 \leq \eta \leq M_1 \text{ for } \zeta = 1, L_1 \end{matrix} \quad (31)$$

(iii) **Temperature**

$$T(\zeta, \eta) = T_{wall} \cdot \begin{matrix} 1 \leq \zeta \leq L_1 \text{ for } \eta = 1, M_1 \\ 1 \leq \eta \leq M_1 \text{ for } \zeta = 1, L_1 \end{matrix} \quad (32)$$

(iv) **Reactant Weight-Fraction**

Note that the transformation parameters are as follows

$$\begin{matrix} \alpha = x_\eta^2 + y_\eta^2 & U = y_\eta u - x_\eta v \\ \beta = x_\zeta x_\eta + y_\zeta y_\eta & V = x_\zeta v - y_\zeta u \\ \gamma = x_\zeta^2 + y_\zeta^2 & W = Jw \\ J = x_\zeta y_\eta - x_\eta y_\zeta \end{matrix} \quad (33)$$

DISCRETIZATION OF TRANSFORMED EQUATIONS

For a non-orthogonal grid system, the best grid configuration is a modified classical staggered-grid (Figure 2) in which both components of u and v velocities are used coincidentally at the same location with the contra-variant velocities normal and parallel to the faces of the cell [16].

The transformed governing equations are discretized using the method known as the control-volume approach [17,18]. The upwind difference scheme is used for discretization of convective terms and the central difference scheme is used for discretization of diffusion terms. The discretization equations are algebraic equations and are solved by a line-by-line tridiagonal matrix (TDMA) algorithm. For the proper location of the control-volume faces, the B-type grid is employed here [18]. The SIMPLER algorithm handles the pressure-velocity coupling in the transverse direction after being modified for the orthogonal coordinate system and non-Newtonian fluids. The method adopted in this work to handle the pressure-velocity coupling in

TABLE 1. Fluid Properties Data.

Properties	Correlation	Units
Density	$\rho = 1174.7 - 0.918T + (75.3 + 0.313T)W_p$	$\frac{\text{kg}}{\text{m}^3}$
Viscosity	$\eta_0 = \exp[-13.04 + 2013/T + MW^{0.18} \times [3.915w_p - 5.437w_p^2 + (0.623 + 1387/T)w_p^3]]$	Pa-s
Thermal Conductivities	$k_m = [2.72 - 2.8 \times 10^{-3}(T - 150) + 1.6 \times 10^{-5}(T - 150)^2](10^{-4})(418.4)$ $k_p = [2.93 + 5.17 \times 10^{-3}(T - 80)](10^{-4})(418.4)$ $k_{\text{mix}} = (1 - X_m)k_m + X_mk_p$	$\frac{\text{J}}{(\text{m})(\text{s})(\text{K})}$ $\frac{\text{J}}{(\text{m})(\text{s})(\text{K})}$ $\frac{\text{J}}{(\text{m})(\text{s})(\text{K})}$
Specific Heat	$C_p = 1880.0$	$\frac{\text{J}}{\text{kgK}}$
Mass Diffusivity	$D_m = 2.0 \times 10^{-9}$	$\frac{\text{m}^2}{\text{s}}$
Heat of Reaction	$\Delta H = -6.7 \times 10^5$	$\frac{\text{J}}{\text{kg}}$
Power Law Index	$n = 0.2$	$\frac{\text{J}}{\text{kg}}$

the axial direction is that of Raithby and Schneider [19].

RESULTS AND DISCUSSION

In this study the thermal polymerization of styrene is analyzed in noncircular cross-sectional duct reactors. The rate equation for this reaction [7-10], considering third-order thermal initiation is expressed by:

$$R_p = \left(\frac{k_p}{k_t^2} \right) (2k_i)^{\frac{1}{2}} (M)^{2.5} \quad (34)$$

in which

$$k_i = 2.019 \times 10^1 e^{(-13810/T)} \frac{\text{m}^6}{(\text{kg})^2 (\text{s})} \quad (35)$$

$$k_p = 1.009 \times 10^5 e^{(-3557/T)} \frac{\text{m}^3}{(\text{kg})(\text{s})} \quad (36)$$

$$k_{tr,m} = 2.218 \times 10^4 e^{(-6377/T)} \frac{\text{m}^3}{(\text{kg})(\text{s})} \quad (37)$$

$$k_t = 1.205 \times 10^7 e^{(-844/T)} e^{[-2(A_1w_p + A_2w_p^2 + A_3w_p^3)]} \frac{\text{m}^3}{(\text{kg})(\text{s})} \quad (38)$$

where

$$\begin{aligned} A_1 &= 2.57 - 5.05 \times 10^{-3}T \\ A_2 &= 9.56 - 1.76 \times 10^{-2}T \\ A_3 &= -3.03 + 7.85 \times 10^{-3}T - 3.03 \end{aligned} \quad (39)$$

The physical properties of the system are shown in Table1. The system model and computer codes are validated in the following section (i) to (iii). There exists a close agreement between the simulation results of the previous investigators and the present simulation study.

The effect of free convection in this study is ignored for the results to be comparable with literature data in which this effect is not considered. Further investigations, which are presented in the following pages, show that conversion results are only negligibly affected if free convection is considered. The effect of variation of number of stations in the axial direction is indicated for two cases, which show a. satisfactorily close agreement in the results of conversion.

Section (i) Husain and Hamielec [3]:

- length of tube: 500 cm
- tube radius: 2.0 cm
- inlet velocity: 0.0695 cm/sec
- inlet/wall temperature: 100°C /100°C
- conversion: 1.26 wt % (for 100 cm tube length)
- conversion: 3.95 wt % (for 300 cm tube length).
- conversion: 6.62 wt % (for 500 cm tube length).

The results obtained in the present analysis are as follows:

(for 5 stations selected in axial direction)

- conversion: 1.38 wt % (for 100 cm tube length)
 - conversion: 4.14 wt % (for 300 cm tube length)
 - conversion: 6.74 wt % (for 500 cm tube length)
- (for 10 stations selected in axial direction)
- conversion: 1.37 wt % (for 100 cm tube length)
 - conversion: 3.95 wt % (for 300 cm tube length)
 - conversion: 6.43 wt % (for 500 cm tube length)

These results are in good agreement with the results of Husain and Hamielec [3] who validated their analysis by experimental data of Wallis [3], which included both chemically and thermally, initiated polymerization of styrene.

Section (ii) Chi-Chi Chen [7]:

- length of tube: 6.4 cm
- tube radius: 0.55 cm
- mass flow: 1.345×10^{-4} kg/sec
- inlet/wall temperature: 140°C / 135°C
- conversion: 26.49 wt%.

The result obtained in the present study is 26.6 wt % conversion which is close to the result obtained above.

Section (iii) Kleinstreuer and Agarwal [9]:

- length of tube: 5.0 m
- tube radius: 2 cm
- mass flow: 0.00002 kg/sec
- inlet /wall temperature: 130°C/100°C

- conversion: 54.8 wt %
- velocity profile: parabolic

The results obtained in the present study are 55.35 wt % and 55.22 wt % for parabolic and uniform velocity profiles respectively.

Following to the validation of the system modeling and computer code, the simultaneous flow, heat and mass transfer problem was solved for thermal polymerization reactors with different cross-sectional geometries, employing 5 sets of operating conditions indicated in Table 2.

The selection of duct geometries of interest and even the angles and side-lengths of some of them is a matter with infinite choices. However, some standard geometries were selected as there was no preference to choose a specific one. These configurations are as follows:

- circular duct,
- square duct,
- equilateral triangular duct,
- trapezoidal duct (acute angle = 60°, one side twice the other),
- pentagonal duct (each angle = 108°)
- hexagonal duct (each angle = 120°)
- rectangular duct (aspect ratio 1.5)
- rectangular duct (aspect ratio: 2.0)

These geometries are shown in Figure 3.

For the sake of numerical accuracy and computational economy a 21x21 grid was selected in transverse direction. The CPU time was about 10 minutes for one run on IBM ESA9000 machine. About 5 iterations were required

TABLE 2. Operating Conditions.

Case	W_{inlet} (m/s)	T_{inlet} (°C)	T_{wall} (°C)	Mass-flow (kg/s)	Reactor Length (m)
# 1	0.000695	100	100	0.7267×10^{-3}	5.0
# 2	0.000695	130	100	0.7027×10^{-3}	5.0
# 3	0.001780	140	135	0.1345×10^{-3}	6.4
# 4	0.000020	130	100	0.2000×10^{-4}	5.0
# 5	0.047250	160	160	0.6095×10^{-3}	14.6

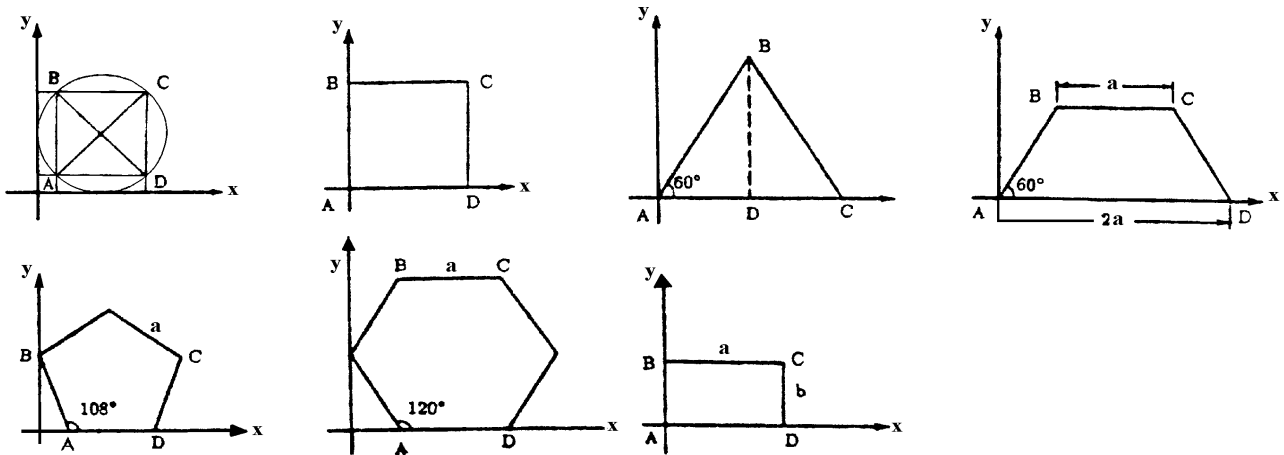


Figure 3. The selected geometries in physical domain (a, b, c, d, e, f, g).

on each transformed-plane for convergence. The convergence criteria were set on the residual values defined as follows:

- (i) The residual of species continuity equation, that is, the remainder of this equation when the result is substituted for mass-fraction into this equation. In general $R = \sum a_{nb} \phi_{nb} + b - a p \phi_p$ and "R" will be zero when the discretization equation is satisfied.
- (ii) The residual of mass-fractions is the difference in mass-fraction values between two successive iterations.

The residual values obtained at convergence in this study were as follows:

- species continuity equation residual: 0.2×10^{-7}
- mass fraction residual: 0.2×10^{-2}

The basis for computations in all the reactors bearing different geometries in their cross-sections and the same length is the same residence-time in the reactors or the same cross-sectional area, while the same uniform velocity is maintained at the inlet of each reactor. The diameter of circular duct corresponding to the cases under study is shown in Table 3.

The results obtained in this analysis are indicated in Tables 4 to 8 for the five cases under consideration. In these tables the results of average polymer weight fraction (WPA) in wt % molecular weights (\bar{M}_n and \bar{M}_w), polydispersity (\bar{M}_w/\bar{M}_n) and bulk-temperature ($^{\circ}\text{C}$) are indicated which are corresponding to the conditions at the exit of the reactors. The total pressure-drop results of the reactors are also indicated. It is observed from these tables that there are only slight differences in the results of conversion obtained for different geometries corresponding to each case. Also the following geometries are observed to provide the maximum conversion for each case:

- Case # 1: circular duct (WPA=6.74 wt%; DP = 1.46 Pa).
hexagonal duct (WPA=6.74 wt%; DP = 1.69Pa).
- Case # 2: circular duct (WPA=14.2 wt%)
- Case # 3: circular duct (WPA=26.6 wt%)
- Case # 4: square duct (WPA=57.2 wt%, DP=9078 Pa)
circular duct (WPA=55.2 wt %; DP=2617Pa).
- Case # 5: 2/1 aspect ratio rectangular (WPA=10.70 wt%; DP=106.6 Pa)
circular duct (WPA=10.10 wt%; DP=50.8 Pa).

TABLE 3. Diameter of Circular-Ducts Corresponding to Non-Circular Geometries.

Cases	#1	#2	#3	#4	#5
Diameter (m)	0.0400	0.0400	0.0110	0.0400	0.00460

**TABLE 4. Simulation Results of Styrene Polymerization at Reactor Exit:
Case # 1.**

No	Geometry	WPA (wt %)	\bar{M}_n ($\frac{\text{kg}}{\text{kg}\cdot\text{mol}}$)	\bar{M}_w ($\frac{\text{kg}}{\text{kg}\cdot\text{mol}}$)	Polydispersity $\frac{\bar{M}_w}{\bar{M}_n}$	Bulk-Temp. (°C)	Total DP (Pa)
1	Circular	6.74	452460	819590	1.81	102.3	1.46
2	Square	6.74	452910	820240	1.81	102.2	1.88
3	Triangular	6.38	453450	820660	1.81	101.9	2.70
4	Trapezoidal	6.33	454100	822100	1.81	101.9	2.57
5	Pentagonal	6.63	453810	822110	1.81	102.1	2.28
6	Hexagonal	6.74	452940	820450	1.81	102.3	1.69
7	Rectangular (AR = 1.5)	6.70	453784	821697	1.81	102.0	1.91
8	Rectangular (AR = 2.0)	6.63	455120	823870	1.81	101.8	1.97

**TABLE 5. Simulation Results of Styrene Polymerization at Reactor Exit:
Case # 2.**

No	Geometry	WPA (wt %)	\bar{M}_n ($\frac{\text{kg}}{\text{kg}\cdot\text{mol}}$)	\bar{M}_w ($\frac{\text{kg}}{\text{kg}\cdot\text{mol}}$)	Polydispersity $\frac{\bar{M}_w}{\bar{M}_n}$	Bulk-Temp. (°C)	Total DP (Pa)
1	Circular	14.2	338740	610770	1.8	106.0	1.05
2	Square	12.7	348550	628480	1.8	104.7	2.52
3	Triangular	11.0	351450	634420	1.8	103.7	6.11
4	Trapezoidal	11.3	352080	635670	1.8	103.7	6.36
5	Pentagonal	12.8	347180	625660	1.8	105.0	2.87
6	Hexagonal	13.6	343910	620230	1.8	105.4	2.76
7	Rectangular (AR = 1.5)	12.2	351620	634550	1.8	104.1	2.80
8	Rectangular (AR = 2.0)	11.5	356170	643600	1.8	103.3	3.26

**TABLE 6. Simulation Results of Styrene Polymerization at Reactor Exit:
Case # 3.**

No	Geometry	WPA (wt %)	\bar{M}_n ($\frac{\text{kg}}{\text{kg}\cdot\text{mol}}$)	\bar{M}_w ($\frac{\text{kg}}{\text{kg}\cdot\text{mol}}$)	Polydispersity $\frac{\bar{M}_w}{\bar{M}_n}$	Bulk-Temp. (°C)	Total DP (Pa)
1	Circular	26.6	220716	392673	1.78	136.3	243
2	Square	26.2	221160	393250	1.78	136.1	244
3	Triangular	24.8	220210	391120	1.78	136.0	347
4	Trapezoidal	25.4	220880	392530	1.78	136.0	347
5	Pentagonal	25.8	220420	391860	1.78	136.2	286
6	Hexagonal	26.5	220910	392960	1.78	136.2	254
7	Rectangular (AR = 1.5)	25.9	221278	393410	1.78	136.0	242
8	Rectangular (AR = 2.0)	25.8	221610	393980	1.78	135.9	261

**TABLE 7. Simulation Results of Styrene Polymerization at Reactor Exit:
Case # 4.**

No	Geometry	WPA (wt %)	\bar{M}_n ($\frac{\text{kg}}{\text{kg}\cdot\text{mol}}$)	\bar{M}_w ($\frac{\text{kg}}{\text{kg}\cdot\text{mol}}$)	Polydispersity $\frac{\bar{M}_w}{\bar{M}_n}$	Bulk-temp (°C)	Total DP (Pa)
1	Circular	55.2	481130	966680	2.00	101.4	2617
2	Square	57.2	499470	998160	2.00	101.2	9078
3	Triangular	47.4	486550	940300	1.93	101.1	11540
4	Trapezoidal	50.0	489210	953850	1.95	101.2	3625
5	Pentagonal	54.8	492120	979150	1.99	101.2	41568
6	Hexagonal	55.7	487320	976770	2.00	101.4	7574
7	Rectangular (AR = 1.5)	54.1	495730	979780	1.98	101.2	4937
8	Rectangular (AR = 2.0)	48.9	488230	947800	1.94	101.1	1910

**TABLE 8 . Simulation Results of Styrene Polymerization at Reactor Exit:
Case # 5.**

No	Geometry	WPA (wt %)	\bar{M}_n ($\frac{\text{kg}}{\text{kg}\cdot\text{mol}}$)	\bar{M}_w ($\frac{\text{kg}}{\text{kg}\cdot\text{mol}}$)	Polydispersity $\frac{\bar{M}_w}{\bar{M}_n}$	Bulk-temp (°C)	Total DP (Pa)
1	Circular	10.10	129960	225290	1.73	161.0	50.8
2	Square	9.97	130040	225440	1.73	160.9	67.2
3	Triangular	10.56	130330	225810	1.73	160.8	106.1
4	Trapezoidal	10.30	130380	226000	1.73	160.8	117.0
5	Pentagonal	10.20	130132	225600	1.73	160.9	67.8
6	Hexagonal	10.40	130100	225570	1.73	161.0	64.1
7	Rectangular (AR = 1.5)	10.20	130250	225810	1.73	160.8	73.9
8	Rectangular (AR = 2.0)	10.70	130430	226000	1.73	160.7	106.6

Therefore, not a specific geometry is recognized to be generally superior to circular duct reactor for the highest conversion of the chemical reaction under study, considering the least pressure-drop results also. The higher pressure-drop of noncircular duct reactors is due to the effect of corners at which the viscosity is tremendously high as observed from the viscosity profile results.

Referring to Tables 4-8, the following relative classification is possible from the conversion point of view based on the circular duct (wt %) results:

Case # 1: 6.74 wt %. low conversion

Case # 2: 14.20 wt %. low conversion

Case # 3: 26.60 wt % intermediate conversion.

Case # 4: 55.20 wt % high conversion.

Case # 5: 10.10 wt % low conversion.

The reason for the low DP results of cases # 1

and # 2 is due to the low level of conversion involved. The relatively higher values of DP of case #5, which is even at low conversion level, is due to the smaller tube I.D. (0.0046 m) practiced in this case. Typical simulation results for molecular-weights distribution, velocity, temperature, concentration, density and viscosity profiles are presented in Figures 4 to 15 in this section.

An analysis of these figures reveals the following major points:

(i) Mol. wt. Distribution All cases except case # 4 (high conversion case) exhibit a peak at a point closer to the reactor inlet. In case # 4, there is a gradual increase in mol wt. distribution from inlet to the end of the reactor. The results are not conclusive to a generalization. The peak is due to

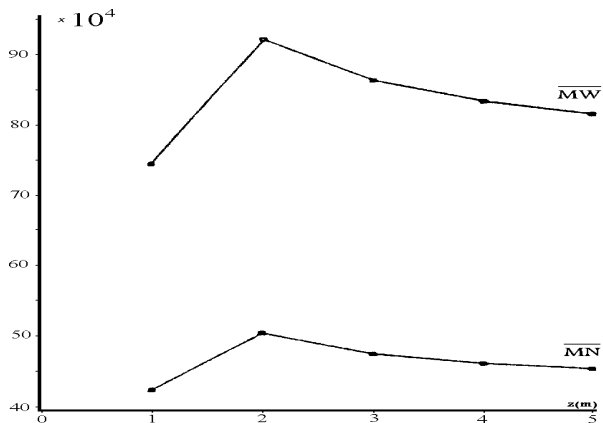


Figure 4. Case#1 mol. wt distribution (triangle).

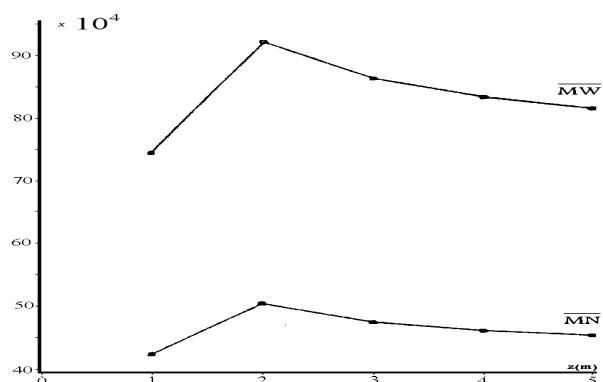


Figure 5. Case#1 mol. wt distribution (trapezoid).

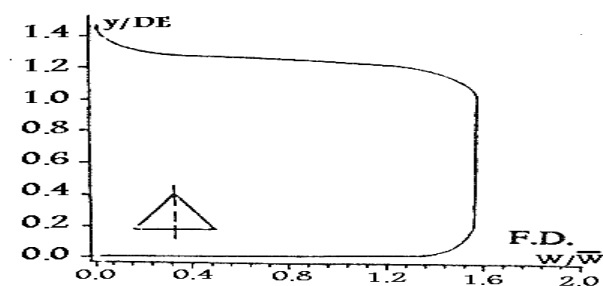


Figure 6. Case#1 axial-velocity profile (triangle).

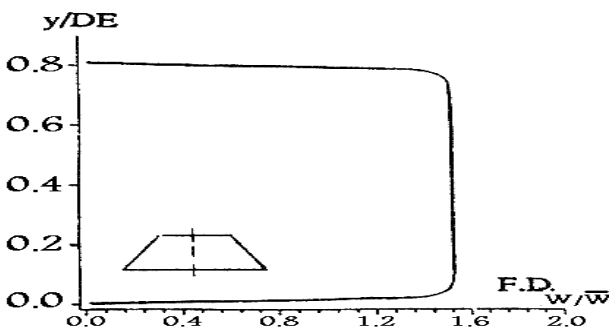


Figure 7. Case#1 axial-velocity profile (trapezoid).

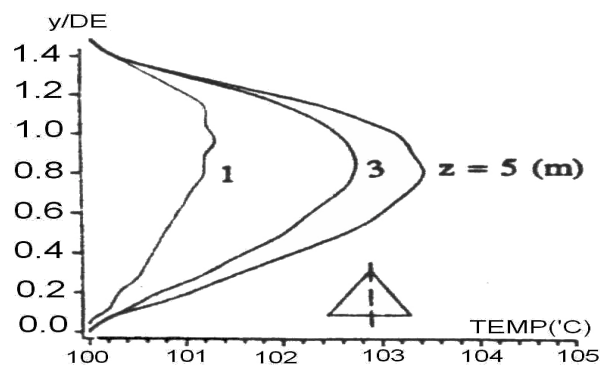


Figure 8. Case#1 temperature profile (triangle).

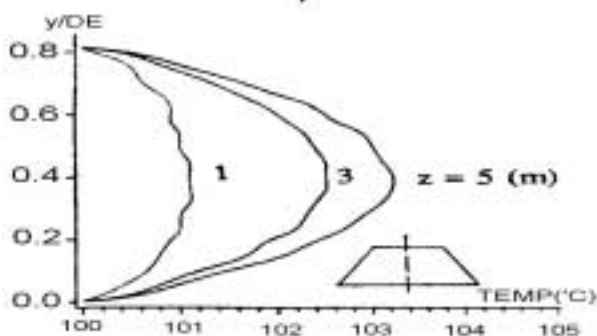


Figure 9. Case#1 temperature profile (trapezoid).

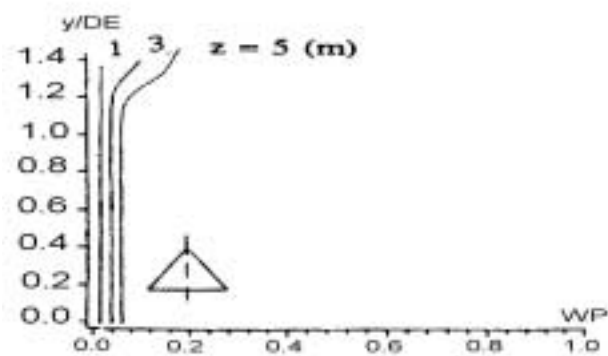


Figure 10. Case#1 polymer-concentration profile (triangle).

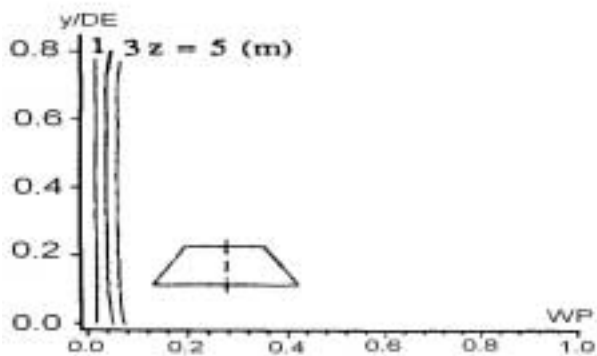


Figure 11. Case#1 polymer-concentration profile (trapezoid).

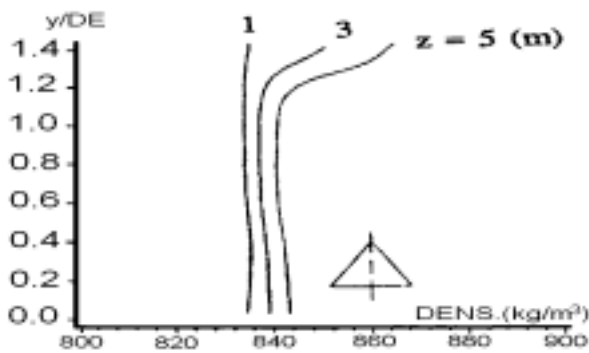


Figure 12. Case#1 density-profile (triangle).

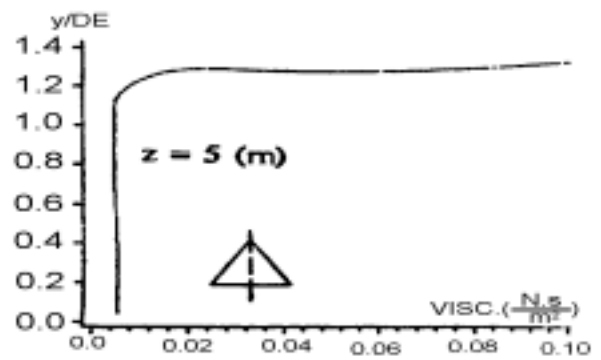


Figure 14. Case#1 viscosity-profile (triangle).

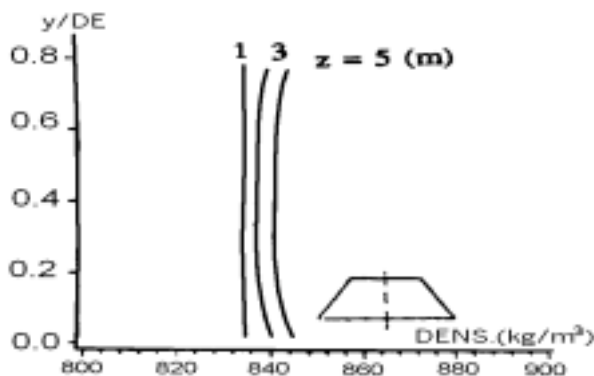


Figure 13. Case#1 density-profile (trapezoid).

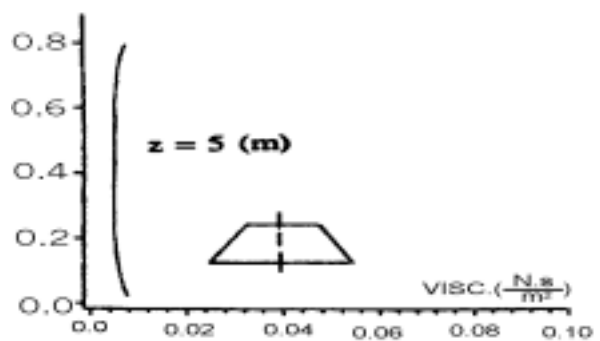


Figure 15. Case#1 viscosity-profile (trapezoid).

the fact that temperature is more uniform transversally at locations closer to the inlet of the reactor due to which the finest quality of polymer is obtained. At downstream locations, however, due to the accumulation of exothermic heat of reaction around the center of the ducts, a non-uniform temperature distribution is generated in transversal-direction, which deteriorates the quality of the polymer product. This is observed by a thereafter-streamwise reduction in the molecular weight results. Typical mol. wt. distributions are shown in Figures 4 and 5 for triangular and trapezoidal duct reactors.

(ii) Axial Velocity Profile All cases exhibit plug flow behavior which is in close agreement with the prediction of Husain and Hamielec [3]. Some velocity distortion is observed due to the effect of angles as revealed in triangular and pentagonal ducts. This effect is to induce higher rates of generation of polymers at corners rather than at sides due to which the viscosity increases around locations closer to angles. The effect on velocity is a retardation of

velocity profile in the vicinity of the angles. Typical axial-velocity profiles are shown in Figures 7 and 8 for triangular and trapezoidal duct reactors.

(iii) Temperature Profiles

Case # 1: Isothermal reactor exothermic reaction proceeds and the temperature profile is developing to higher values.

Case # 2: Cooled-wall reactor, heat removal is observed from the temperature profile, which is developing to lower values.

Case # 3: Mildly cooled-wall reactor, temperature profile is mildly developing to lower values.

Case # 4: Cooled-wall reactor, temperature profile is developing to lower values.

Case # 5: Isothermal reactor, temperature profile is developing to higher values.

Typical temperature profiles are shown in Figures 8 and 9 for triangular and trapezoidal duct reactors.

(iv) Concentration Profile The profiles are developing. Referring to angle effect, such as for

triangular and pentagonal ducts, an increase in concentration is observed at these locations. Typical concentration profiles are shown in Figures 10 and 11 for triangular and trapezoidal duct reactors.

(v) Density and viscosity profiles The effect of angles, is plainly observed in viscosity profiles such that there is a drastic increase in viscosity close to the angles. This is observed in viscosity profiles for the triangular and pentagonal ducts of all cases. The density profiles are also affected to some extent close to these points. The angle effect is the reason for the higher pressure-drop of noncircular duct reactors relative to the circular ones. Typical density and viscosity profiles are shown in Figures 12 to 15 for triangular and trapezoidal duct reactors.

Effect of Free-Convection Due to the narrow temperature range involved in the transverse direction, the effect of free-convection (buoyancy effect) in this study is found to be negligible. This is observed from the following results, which were obtained, considering free-convection effect for circular ducts corresponding to the results in Tables 4-8.

Case # 1: 6.75 wt % conversion.

Case # 2: 14.50 wt % conversion.

Case # 3: 26.70 wt % conversion.

Case # 4: 55.24 wt % conversion.

Case # 5: 10.30 wt % conversion.

SUMMARY AND CONCLUSIONS

This paper shows the suitability of a non-orthogonal boundary-fitted coordinate transformation method in the solution of 3D parabolized mass, momentum, energy and species continuity equations in laminar flow and in reacting media in arbitrary cross-sectional duct reactors. The favorable agreement obtained between this numerical solution procedure with the results of other investigators for circular ducts and the absence of convergence difficulties prove the elegant feature of the above-mentioned method. As a novel idea in reaction engineering, the above solution technique is employed to analyze the simulation of styrene polymerization in arbitrary cross-sectional duct reactors. It is observed that not a specific geometry is in general superior than the conventional circular duct reactors considering also the least pressure-drop in the reactors.

NOMENCLATURE

a	coefficient in the discretization equation
b	constant term in the discretization equations
C_p	specific heat
D.L.	dimensionless
D A	mass diffusivity of "A"
$D_{h,DE}$	hydraulic diameter (or equivalent diameter)
F.D.	fully developed
g	acceleration due to gravity
I	index of "ζ" axis in the transformed plane
J	index of "η" axis in the transformed plane
J	Jacobian of transformation
k	thermal conductivity
k_i	rate constant for thermal initiation
k_p	rate constant for propagation
$k_{tr,m}$	rate constant for chain transfer to monomer
k_t	rate constant for termination
[M]	monomer concentration
M	apparent viscosity for power-law fluid
m, m_A	monomer (A) weight—fraction
$\overline{M}_n, \overline{M}_n$	cup average number averaged molecular weight
$\overline{M}_w, \overline{M}_w$	cup average weight averaged molecular weight
n	Power-law index
n	unit normal vector
P	total pressure (dynamic + hydrostatic)
P	dynamic pressure
-	
P	mean viscous pressure
q	heat flux
Q_R	heat of reaction
R	residual of discretization equation
R_A	mass rate of consumption of reactant "A" due to chemical reaction
R_p	rate of polymerization
T	temperature
u, v, w	velocity components in the Cartesian system
U, V, W	contra variant velocity components
v	velocity field
WPA	average polymer weight fraction
w_i	inlet velocity

\bar{W}	mean axial velocity
x, y, z	Cartesian coordinate system
X_m	monomer conversion
z	reactor length

Greek Letters

ΔH	heat of reaction
α, β, γ	coordinate transformation coefficients
$\varepsilon, \eta, \sigma$	axes of curvilinear coordinate
μ	consistency index (for power-law fluids)
ρ	density
ρ_a	arithmetic mean density for duct cross— section
Δ_{ij}	rate of deformation tensor
τ_{ij}	stress-tensor
Φ_v	viscous dissipation function
η_o	viscosity
ϕ	a general dependent variable

Subscripts

nb	General neighbor grid point
----	-----------------------------

REFERENCES

- Sala, R., Valz-Gris, F. and Zanderighi, L., "A Fluid-Dynamic Study of a Continuous Polymerization Reactor", *Chemical Engineering Science*, 29, (1974), 2205-2212.
- Wyman, C. E. and Carter, L. F., "A Numerical Model for Tubular Polymerization Reactors", *AIChE Symposium Series*, Vol. 72, No. 160, (1976), 1-16.
- Husain, A. and Hamielec, A. E., "Bulk Thermal Polymerization of Styrene in a Tubular Reactor—a Computer Study", *AIChE Symposium Series*, Vol. 72, No. 160, (1976), 112-127.
- Hui, A. and Hamielec, A. E., "Thermal Polymerization of Styrene at High Conversions and Temperatures, An Experimental Study", *J. Appl. Polymer Science*, 16, (1972), 749-762.
- Valsamis, L. and Biesenberger, J. A., "Continuous Bulk Polymerization in Tubes", *AIChE Symposium Series*, Vol. 72, No. 160, (1976), 18-27.
- Valsamis, L., and Biesenberger, J. A., "Continuous Bulk Polymerization of Styrene in a Tubular Reactor", *AIChE Annual Meeting*, N. Y., N. Y., (1977).
- Chen, C. C., "Polymerization in a Laminar Flow Tubular Reactor", Ph. D. Thesis, Rensselaer Polytechnic Institute, Troy, N. J., (1986).
- Chen, C. C. and Nauman, E. B., "Verification of a Complex, Variable Viscosity Model for a Tubular Polymerization Reactor", *Chemical Engineering Science*, 44, No. 1, (1989), 179-188.
- Kleinstreuer, C. and Agarwal, S., "Coupled Heat and Mass Transfer in Laminar Flow, Tubular Polymerizers", *Int. J. Heat Mass Transfer*, 29, No. 7, (1986), 979-986.
- Agarwal, S. S. and Kleinstreuer, C., "Analysis of Styrene Polymerization in a Continuous Flow Tubular Reactor", *Chemical Engineering Science*, 41, No. 12, (1986), 2101-3110.
- Isazadeh, M. A., "Numerical Solution of Reacting Laminar Flow Heat and Mass Transfer in Ducts of Arbitrary Cross-Sections for Power-Law Fluids", Ph.D. Thesis, McGill University, Montreal, Canada, (1993).
- Bird, R. B., Stewart, W. E. and Lightfoot, E. N., "Transport Phenomena", Wiley, New York, (1960).
- Skelland, A. H. P., "Non-Newtonian Flow and Heat-Transfer", John Wiley and Sons, NY., (1967).
- Chu, W. H., "Development of a General Finite Difference Approximation for a General Domain", *J. Comp. Physics*, 8, (1971), 392-408.
- Thompson, J. F., Thames, F. C. and Mastin, C. W., "Boundary-Fitted Curvilinear Coordinate Systems for Solution of Partial Differential Equations on Fields Containing Any Number of Arbitrary Two-Dimensional Bodies", *Report CR-2729, NASA Langley Research Center*, (1977).
- Maliska, C. R. and Raithby, C. D., "A Method for Computing Three Dimensional Flow Using Non-Orthogonal Boundary—Fitted Coordinates", *Int. J. for Numerical Methods in Fluids*, 4, (1984), 519-537.
- Patankar, S. V. and Spalding, D. B., "A Calculation Procedure for Heat, Mass and Momentum Transfer in Three-Dimensional Parabolic Flows", *Int. J. Heat Mass Transfer*, 15, (1972), 1787-1806.
- Patankar, S. V., "Numerical Heat Transfer and Fluid Flow", Hemisphere Publishing Corporation, NY., (1980).
- Raithby, G. D. and Schneider, G. E., "Numerical Solution of Problems in Incompressible Fluid Flow: Treatment of the Velocity-Pressure Coupling", *Numerical Heat Transfer*, 2, (1979), 417-440.